Climate and land-use changes drive taxonomic and functional biodiversity through time

Authors: S. Marta[1*], M. Brunetti[2], R. Manenti[1], A. Provenzale[3] & G.F. Ficetola[1]

Corresponding author: Silvio Marta; e-mail: silvio.marta@hotmail.it; mobile: +39 3779625871;

ORCID ID: https://orcid.org/0000-0001-8850-610X

Affiliations:

1. Department of Environmental Science and Policy, University of Milan, Via G. Celoria 26, 20133 Milan, Italy
2. Institute of Atmospheric Sciences and Climate, ISAC-CNR, Italian National Research Council, 40129, Bologna, Italy
3. Institute of Geosciences and Earth Resources, IGG-CNR, Italian National Research Council, 56124, Pisa, Italy

Abstract

Long-term studies are essential to understand the impacts of global changes on the multiple facets of biological diversity. Here, we report that multiple environmental stressors, namely climate, land-use and human population density jointly acted in conditioning assemblage composition and functionality over long time periods. By carefully reconstructing the temporal evolution of these stressors, we explicitly tested how environmental changes can determine the observed changes in taxonomic and functional diversity. We found that rapid changes in precipitation de-stabilize the assemblages and maximize colonization and extinction rates, especially when coupled with changes in human population density (for taxonomy) or temperature (for functionality). Higher microclimatic heterogeneity increases the stability of biodiversity, by reducing taxonomic and functional loss. Finally, changes in natural habitats increased colonization, influencing taxonomic nestedness and functional replacement. The integration of long-term datasets combining distribution, climate and traits may deepen our understanding of the processes underlying biodiversity responses to global-scale drivers.

Introduction

Ongoing land-use and climate changes represent global threats to biological diversity[1,2]. The rapid growth of the human population, with the resulting increased exploitation of natural resources, has tremendously accelerated the modification of natural systems[3,4]. Rapid climate change, including temperature increases and alterations to precipitation patterns, is leading to multiple impacts on biodiversity[5,6], and often interacts with other global-change stressors[7,8]. The biodiversity dynamics following such changes may have severe consequences on the functioning of ecosystems, including their ability to provide goods and services, and hence potentially leading to adverse impacts on human health, well-being and socio-economic development[9,10].

Biodiversity is a multifaceted concept and a full assessment of the consequences of global changes requires the understanding of impacts on taxonomic diversity (e.g. species richness), but also on evolutionary processes (e.g. phylogenetic diversity) and ecosystem functioning (e.g. functional diversity)[11,12]. Long-term studies are essential to achieve this task, as they allow relating biodiversity trajectories to climate and land-use shifts. However, the scarcity of long-term biodiversity data generally limits the possibility of such analyses, and most of the available studies focus on changes in species richness or phenology[13,14,15].

Temporal β-diversity (i.e., the compositional dissimilarity over two or more time points for the same place) provides a partially unexplored but powerful tool to detect the effects of environmental changes on biological diversity[16,17]. Whereas α-diversity is agnostic to species identity, β-diversity takes explicitly into account assemblage composition, thus providing a more sensitive indicator of biotic changes induced by climate and land-use shifts[17,18]. In addition, β-diversity can be partitioned into turnover and nestedness components, allowing an in-depth analysis of the processes shaping assemblage composition. Temporal turnover reflects species replacement over time, and can be caused by neutral processes, such as chance colonization and ecological drift, or environmental sorting[19]. Temporal nestedness, on the other hand, is the tendency of two

assemblages to be subset of one another, indicating species loss or gain over time as a result of non-random dynamics promoting the compositional depletion or enrichment of the assemblage[16,19,20]. Taxonomic and functional dissimilarities are different facets of biodiversity that can show different responses to environmental changes[16], depending on the redundancy of single species' functional traits within the assemblage: the more original are the traits of a species, the less replaceable will be its contribution to overall functioning[11,21].

Understanding the drivers of biodiversity change through time is pivotal to detect the impacts of global stressors at both the taxonomic and functional levels. Temporal changes in species richness and temporal β-diversity may provide measures of directional shifts in community composition in response to e.g. (micro-)climate, landscape changes or changes in nitrogen deposition[22,23,24]. Positive relationships between the change in a given environmental parameter and β-diversity may result from nestedness caused, for instance, by species loss (particularly the rarest ones) (Fig. 1a-b) or from high rates of compositional turnover with higher environmental change, for instance following temperature increase[25] (Fig. 1c-d). Non-linear (e.g. quadratic) trends centred on zero could instead result from responses that are sensitive only to the magnitude of changes in the environmental driver, independent of its sign (e.g. both precipitation increase and decrease). In this case, the dissimilarity is at its minimum when the change is low and it increases with more profound changes, whatever their sign (Fig. 1e-h). Unfortunately, the scarcity of long-term data has limited our understanding of relationships between environmental change and biodiversity (but see e.g. [18]).

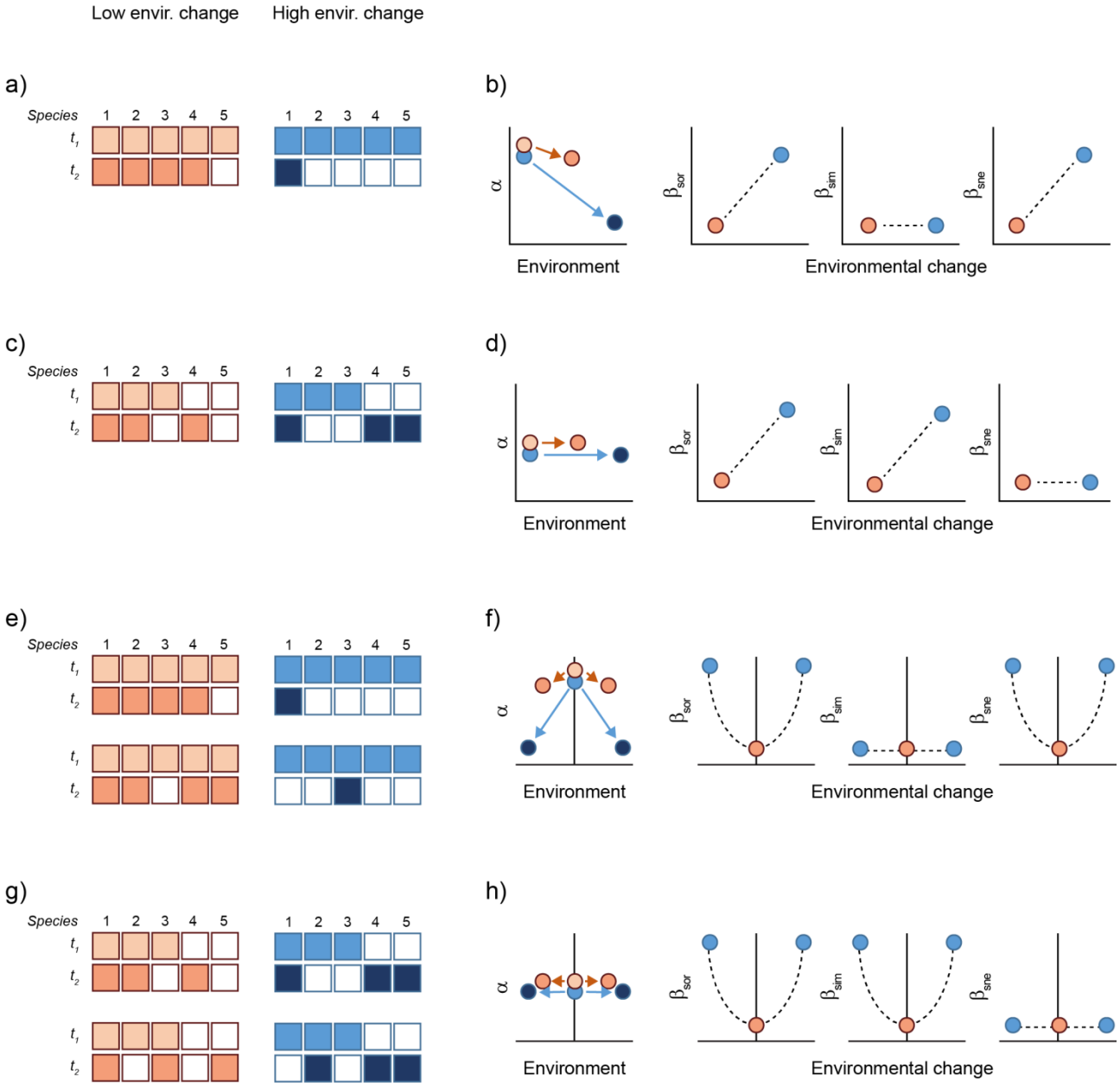

Fig. 1: Potential effects of environmental changes on the α- and β-diversity of assemblages. The effects are exemplified for two assemblages sharing the same pool of species at t_1, but experiencing different intensities of change. a) An environmental change leads to a modification in assemblage composition between t_1 and t_2, with stronger environmental change for the blue assemblage. b) These environmental changes affect biodiversity, leading to loss of α-diversity (strongest for the blue assemblage) and causing higher temporal β-diversity (β_{sor}) in blue, which is attributable to nestedness (β_{sne}). c) In this case, the environmental change causes assemblage modifications that, as shown in d), are reflected by higher temporal β-diversity (β_{sor}) in blue, attributable to turnover (β_{sim}). e and g) For many parameters, the environment can drive changes with different sign (e.g. precipitation can either increase and decrease through time; Fig. 2b), both causing community changes. As shown in f and h), this leads to non-linear relationships between the strength of environmental change and the different components of β-diversity.

Terrestrial arthropods are the most ubiquitous animals on the Earth, exhibiting an astonishing diversity in species, adaptations and life forms and providing multiple ecosystem services[26], notwithstanding they are undergoing dramatic biodiversity shifts and declines because of ongoing global changes[26,27,28,29]. Here we used a unique biodiversity dataset on the Italian fauna covering more than 150 years[30] to unravel the processes determining long-term diversity dynamics of arthropod assemblages at both the taxonomic and functional levels. We integrated multiple information on environmental variations to estimate the relative role of changes in climate, land-use and human population, as well as the effects of microclimatic buffering. Temporal changes in assemblage composition and functionality were measured using the Sørensen dissimilarity, which accounts for both species replacement and differences in α-diversity between spatially or temporally disjoint assemblages[19,31]. To represent the opposite processes of species replacement and loss/gain through time, we partitioned total dissimilarity into the additive components of turnover and nestedness[16,19] and of D_{gain} and D_{loss}[32]. Temporal variations are directional processes (i.e., we study the changes of a given assemblage from t_0 to t_1) and this allows to explicitly link species gains and losses to the fundamental mechanisms (i.e., colonization and extinction) underlying the observed functional and compositional changes. We related the rate of change of dissimilarity and its components to environmental variation, in order to identify the overall response of biological communities to environmental changes and the underlying processes. We expected smaller changes in β-diversity for microclimatically heterogeneous landscapes, due to the stabilizing effect of microclimatic buffering resulting in the reduction of both turnover and / or nestedness[33]. On the other hand, higher rates of climate and land-use changes, promoting more rapid extinction / colonization dynamics due to the coupled effects of human pressure and niche displacement[1], may increase species turnover and / or nestedness, ultimately resulting in local increases of β-diversity.

Results

Climate, land-use and human population changes

After our rigorous cleansing procedure, we obtained high-quality biodiversity data for multiple time periods in 109 cells covering the whole Italian area (Fig. 2). In these cells, the analysis of environmental changes over the entire time series (Supplementary Table 1) clearly showed an increase of mean annual temperature, which became particularly evident in the last five decades (Fig. 2a), and a decrease in annual precipitation (Fig. 2b). The surface covered by natural and semi-natural habitats experienced a decline during the period 1860-1950, followed by a significant rebound during recent decades (Fig. 2c), while human population increased until reaching a plateau after 1980 (Fig. 2d). The mapping of random intercepts identified complex spatial patterns for the environmental variables, with lower temperatures, higher precipitation and more natural habitat in mountain areas (Fig. 2e-g, respectively), and higher human population density in lowlands and nearby the main cities (Fig. 2h).

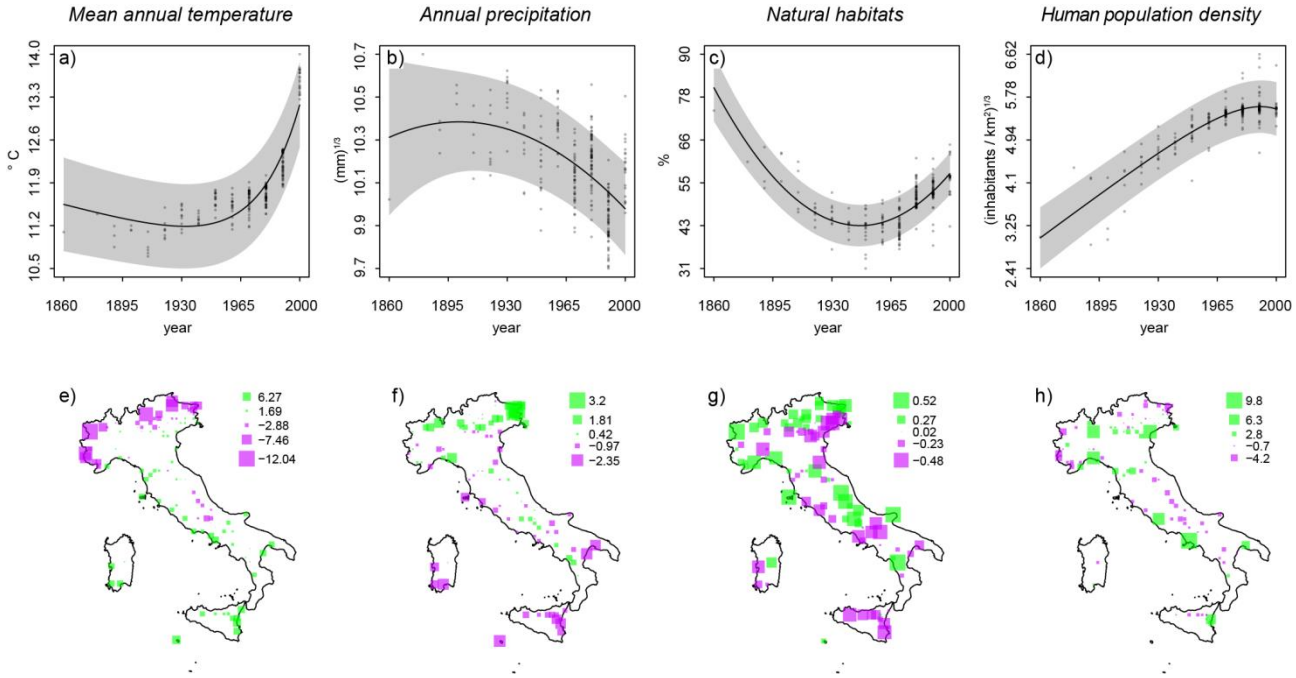

Fig. 2: Temporal evolution of climate, land-use and human population density over the entire time series (1859-2003 CE). Cell identity was introduced as random intercept to take into account the cell-specific conditions influencing climate (e.g., elevation, latitude ...), land-use and human population density (percentage of natural areas or human population density at the beginning of the series). a-d: reconstructed temporal trends (Nakagawa & Schielzeth[92] conditional R^2: 0.99; 0.96; 0.97; 0.99 - marginal R^2: 0.02, 0.01, 0.03, 0.02); grey area represents the 95% confidence interval for the average estimate. Precipitation and human population density are cube-root transformed. e-h: spatial distribution of the random intercepts; purple squares mark negative values (i.e. lower than the average), green squares positive ones. The square size is proportional to the value of the random intercept.

Temporal β-diversity

To identify the processes underlying biodiversity change, average rates of change of dissimilarity and its components were related to the annual rates of change in climate, land-use and human population, and to the average microclimatic heterogeneity within the intervals. We measured β-diversity, nestedness, turnover and scaled gain and loss components between 169 pairs of temporally disjunct assemblages (Chilopoda = 43; Histeridae = 36; Orthoptera = 28; Dytiscidae = 17; Ephemeroptera = 18; Odonata = 27). We accounted for the differences in interval duration by

dividing dissimilarity measures by the interval duration over which they were accumulated. This approach allowed the minimization of the effects that a natural baseline turnover may exert on the overall dissimilarity over long time intervals[34], which conceal the impact of changes in climate or land-use. We also assessed the possibility of non-linear relationships and interactions using the Watanabe-Akaike information criterion (WAIC[35]; see Methods for further details).

The rate of change of taxonomic β-diversity was higher in cells experiencing faster changes in natural habitat, faster (positive or negative) changes in precipitation, slower changes in human population density and lower microclimatic heterogeneity (Fig. 3a). Additionally, we found a strong interaction between precipitation and human population density. The effect of precipitation change was particularly evident in cells where human population increased more rapidly (Fig. 4a-c). Similarly, the rate of change of taxonomic turnover was higher for cells with lower microclimatic heterogeneity, with strong (positive or negative) precipitation changes and with slower changes in human population densities. Also in this case, we found a strong interaction between precipitation and human population changes (Fig. 3b; Supplementary Fig. 1a-c). Conversely, the rate of change of the nestedness component of dissimilarity was highest in cells experiencing rapid increase of natural habitats and small changes in human population density and precipitation. Also in this case, we detected a positive interaction between precipitation and human population change (Fig. 3c; Supplementary Fig. 1d-f), although this effect was weaker than that observed for β-diversity and turnover.

Since functional diversity is known to be sensitive to species richness[36,37], we used P-values based on null models to obtain estimates of functional diversity (both β- and its components) independent of the patterns of richness[37] (see Methods). With this approach, values of functional β-diversity e.g. > 0.5 indicate assemblages that are functionally more dissimilar than expected given their taxonomic dissimilarity. The same holds for the nestedness and turnover components of dissimilarity, as well as for scaled gain and loss components of dissimilarity. The analysis of

changes in functional diversity returned patterns comparable to the changes in taxonomic diversity for β-diversity, turnover and nestedness (Fig. 3d-f). The change in functional β-diversity was more rapid in cells experiencing faster (positive or negative) changes in precipitation, faster temperature changes and lower microclimatic heterogeneity (Fig. 3d). We also found a strong interactive effect between precipitation and temperature. Faster changes in temperature were linked to particularly strong changes in functional β-diversity when precipitation increased (Fig. 4d- f). The change in functional turnover was faster in cells experiencing rapid increase of natural habitat, and rapid (positive or negative) changes in precipitation (Fig. 3e). The interaction between temperature and precipitation changes had a very weak effect on functional turnover (Supplementary Fig. 2a-c). Conversely, the rate of change in functional nestedness was higher in cells with, again, faster (positive or negative) changes in precipitation and temperature (Fig. 3f). In addition, the strong interaction between precipitation and temperature showed that the positive effects of changes in temperature are particularly strong when precipitation rate increased (Supplementary Fig. 2e and f).

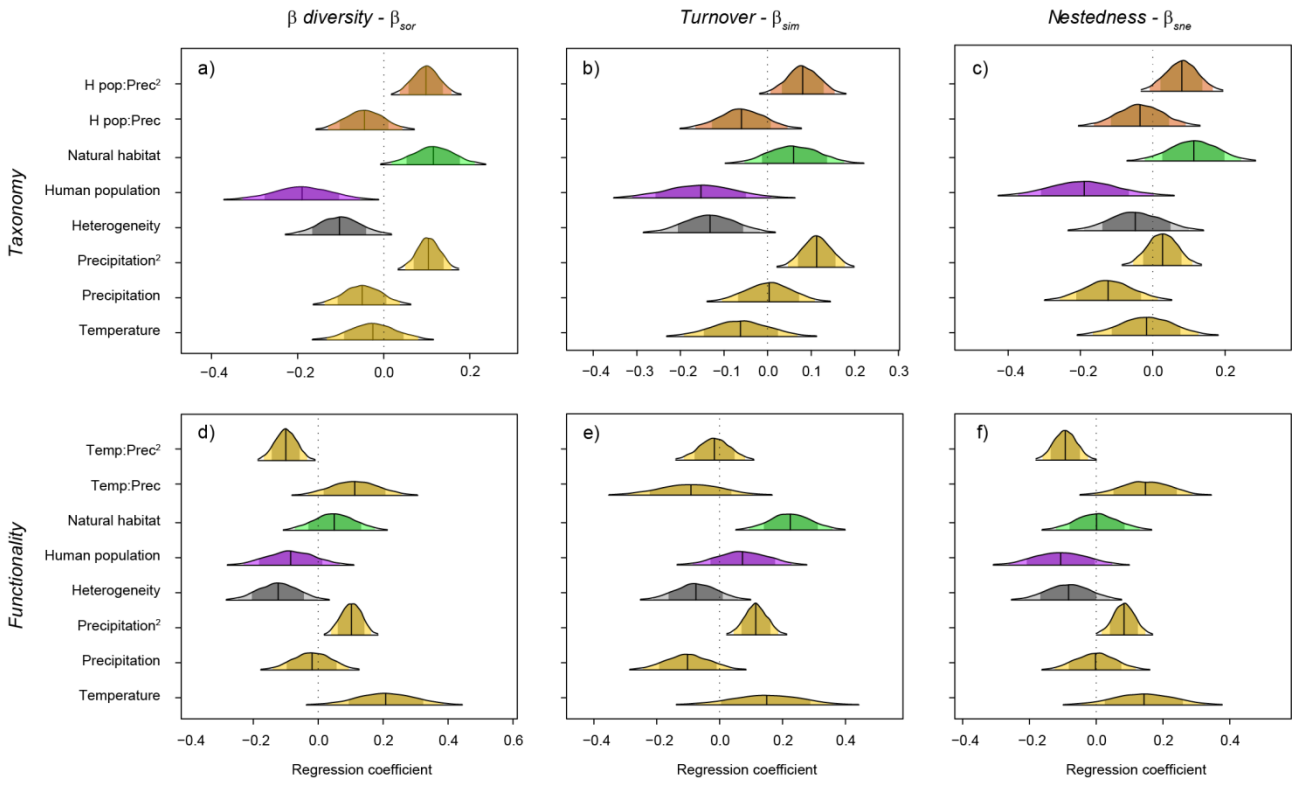

Fig. 3: Density plots of the posterior distribution for the relationships between the rates of change of β-diversity, turnover and nestedness and the candidate environmental drivers. Taxonomy (a-c) vs. functionality (d-f); Sørensen dissimilarity (a and d), temporal turnover (b and e), and temporal nestedness (c and f). The figure represents median values for regression coefficients (vertical lines), and 80 (colours), 95 (pale colours) and 99 % (outlines) credible intervals. Quadratic terms and interactions were only included if supported for β_{Sor} by the Watanabe-Akaike Information Criterion[35]. Interactions: Prec = Annual precipitation; H pop = Human population density; Temp = mean annual temperature.

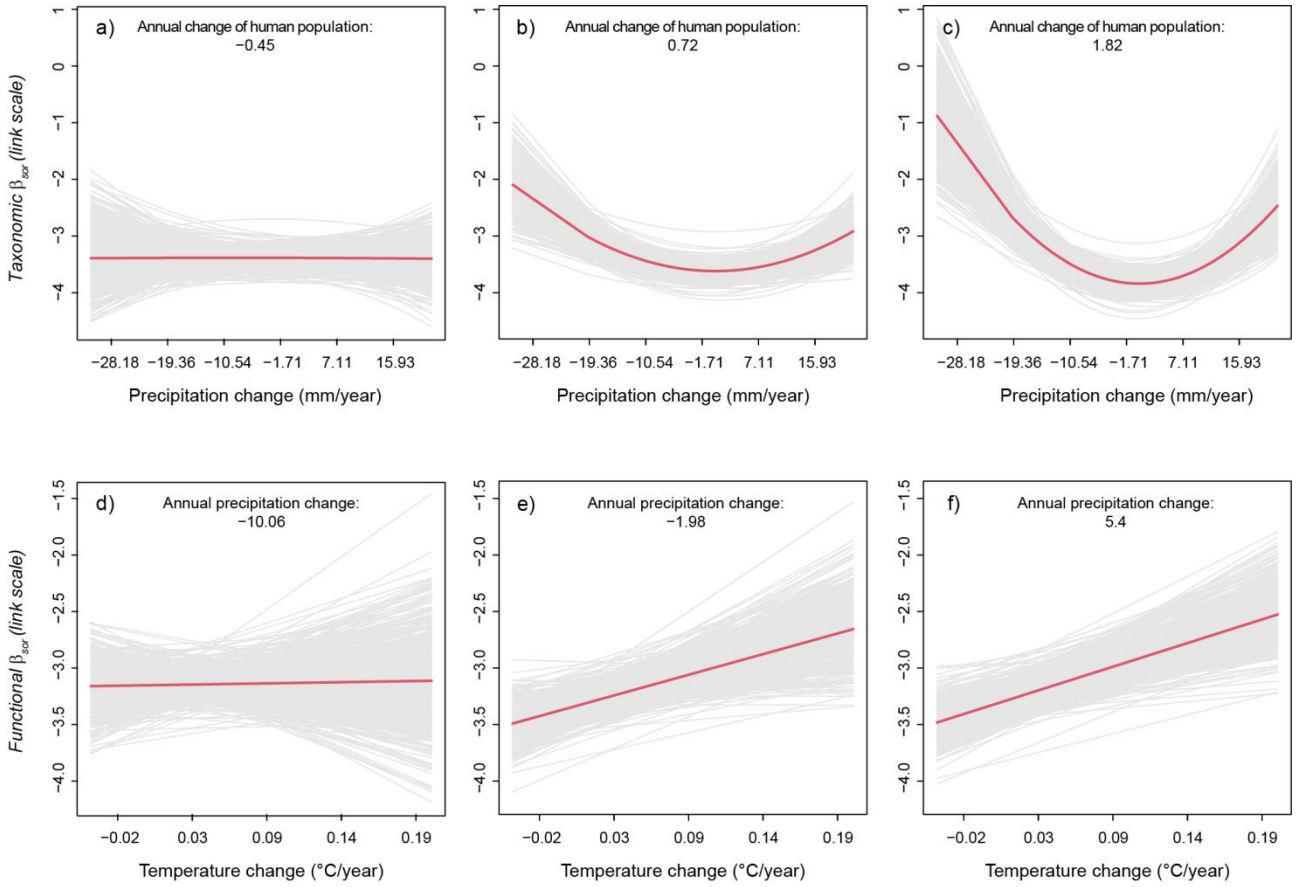

Fig. 4: Relationships between β-diversity and the environmental drivers returning significant interactions. In each plot, the thick red line represents the average predicted relationship on the link scale, while the grey lines represent 500 samples of the posterior distribution. a-c show the effect of precipitation change (mm/year) on taxonomic β-diversity in cells with negative (-0.45), medium (0.72) and rapid (1.82) changes of the human population density (cube-root transformed; $(\text{inhabitants/km}^2\text{/year})^{1/3}$). d-f show the effect of temperature change (°C/year) on functional β-diversity with negative (-10.06), stable (-1.96) and positive (5.4) rates of change in precipitation (mm/year).

To understand the effect of species extinction and colonization on temporal β-diversity and its components (i.e., nestedness and turnover), we further decomposed the Sørensen dissimilarity into scaled gain and loss components (D_{gain} and D_{loss}[32]). Functional losses and gains were estimated by comparing the functional diversity associated to shared, "colonizing" (i.e., newly detected) and "extinct" species (i.e., species not anymore detected), to that expected under a random assignment of traits to species (see Methods). Species gain was faster in cells experiencing rapid increase in natural habitat and fast (positive or negative) precipitation change (Fig. 5a), while increasing human population slowed down species gain. Additionally, the interaction between precipitation and human population changes showed that the effect of precipitation change is particularly strong in cells experiencing rapid increases in human population density (Supplementary Fig. 1h-i). Species loss was faster in cells with low microclimatic heterogeneity, slow change in human population and fast (positive or negative) precipitation changes (Fig. 5b), with the interaction showing the same pattern detected for species gain (Supplementary Fig. 1j-l). The change in functional gain was highest in areas experiencing fast increase of natural habitat, and rapid (positive or negative) precipitation changes. Functional gain was not affected by the interaction between precipitation and temperature (Supplementary Fig. 2g-i). Functional loss was faster in areas experiencing rapid precipitation changes, and characterized by low microclimatic heterogeneity (Fig. 5c and d); as above, no clear interactive effects were identified (Supplementary Fig. 2j-l).

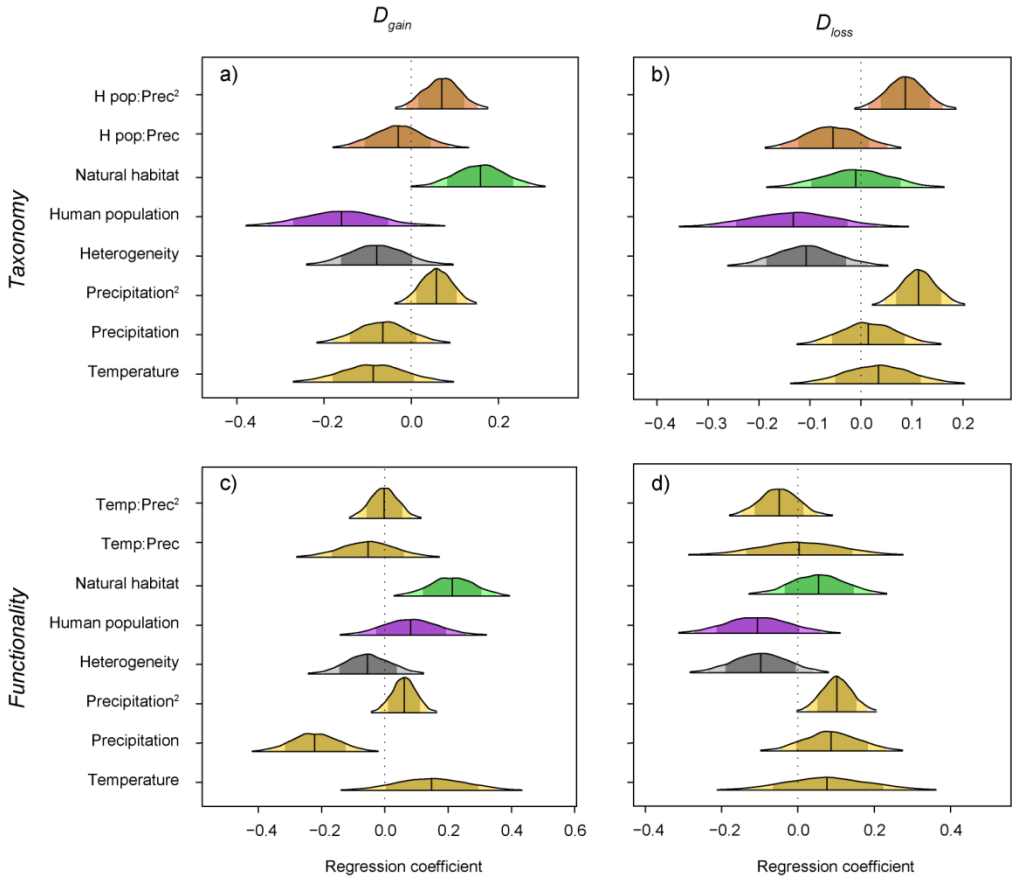

Fig. 5: Density plots of the posterior distribution for the relationships between the rates of change in the scaled gain (D_{gain}) and loss (D_{loss}) components of β-diversity and candidate environmental drivers. Taxonomy (a-b) vs. functionality (c-d); D_{gain} (a and b) and D_{loss} (c and d). The figure represents median values for regression coefficients (vertical lines), and 80 (colours), 95 (pale colours) and 99 % (outlines) credible intervals. Interactions: Prec = Annual precipitation; H pop = Human population density; Temp = mean annual temperature.

Discussion

In recent decades, we have experienced dramatic changes in multiple components of the Earth's systems, ranging from climate to the distribution of habitats and species[9]. These changes are evident in almost all the areas of the world, and understanding their consequences on the different components of biological diversity is a necessary prerequisite for effective management. Our

analyses showed that changes in precipitation, temperature, natural habitats and human population density, together with microclimatic heterogeneity, jointly acted as major drivers of temporal β-diversity and its components, at both the taxonomic and functional levels (Fig. 3 and 4).

The rapid increase in mean annual temperature and the changes in annual precipitation are inducing remarkable transformations in many environments. This is particularly evident in the Mediterranean area, a region identified as a hot spot of climate change, where the strong temperature rise observed in the past decades is expected to continue in the future[38]. In Italy, a country with a long record of environmental investigations and weather observations, the data indicate a stronger-than-average temperature rise and a long-term precipitation decline[39]. These changes have multiple consequences, such as the decrease of mountain snow cover and glaciers[40,41], increase in the intensity of summer heat waves[42], the expected increase of wildfires[43], and multifaceted impacts on species population dynamics[44,45] and protected areas[46].

Given the limited direct records for croplands and pasturelands for the period preceding 1960 CE, we retrieved information about natural habitats from analyses integrating data on human population and per-capita land use[47]. Still, the marked land-use changes detected here for the whole period (Fig. 2c and d) are in line with observations from other European countries, where extensive re-expansion of forests following the abandonment of traditional agricultural areas occurred widely in the late XX century[48]. In Mediterranean countries, such process started earlier and had stronger effects in mountains and other areas where agriculture and pastoralism are less economically-profitable[49]. In the last decades, the human population reached a plateau in most European countries[50], mainly because of a decrease in fertility rate linked to increased welfare levels[51]. The overall scenario of environmental change recorded in the study area during the last 150 years was extremely complex, as it combined periods of strong anthropization with stable periods and even rewilding, coupled with substantial increases in temperature and complex changes in precipitation patterns. Though difficult to disentangle, analysing assemblage responses following these changes may provide a relatively complete picture of the effects of environmental change on biodiversity.

Taxonomic and functional dissimilarities showed coherent responses to climate changes, in terms of both β-diversity and its components (Figs. 3, 4 and 5). Several studies on the impact of climate change on biodiversity have focused on the effects of global warming. Surprisingly, we found limited effects of temperature change alone on β-diversities and their components. Rather, temperature change increased functional turnover when coupled with increased precipitation (Fig. 3e, 4d-f; Supplementary Fig. 2a-c), and determined functional restructuring of the assemblages. Precipitation changes showed the strongest and most consistent contribution to biodiversity change, and frequently interplayed with other parameters. Faster precipitation changes promoted both taxonomic and functional dissimilarity, turnover and, to a lesser extent, nestedness (Fig. 3), with species losses being slightly greater than gains at medium and higher human population densities, possibly as a result of increasing human disturbance[4,7]. Precipitation changes alter water balance, local water availability and nutrient cycling, directly affecting ecosystem productivity and food availability for primary consumers, especially in arid and semi-arid regions[52]. Precipitation changes and water stress may directly or indirectly affect eco-physiological responses of herbivores[53] and some analyses suggest that precipitation changes can have stronger effect on population dynamics[54] or species optimum elevation[55] than temperature changes alone. The effects of precipitation changes and increased drought may be even more pronounced when these changes act synergistically with temperature increases, ultimately leading to widespread tree mortality and vegetation shifts with cascading effects on animal communities and ecosystem functioning[56]. Additionally, precipitation changes frequently interact with other climate[57] or land-use stressors[7,58], shaping the composition and functioning of biological assemblages[2]. Since spatially and temporally explicit projections of precipitation can be difficult to produce, there is a fundamental uncertainty in one of the most important drivers of future ecosystem and population responses, which calls for innovative approaches such as decision-scaling methods[59] that can greatly improve our estimates of ecological responses.

Microclimate heterogeneity buffered the rates of change of β-diversities, taxonomic turnover and functional nestedness (Fig. 3a, b, d and f), owing to a significant decrease of taxonomic and functional losses with increasing heterogeneity (Fig. 5b and d). Heterogeneous microclimates thus stabilized local assemblages by decreasing extinction rate, resulting in a reduction of species replacement over time. This finding stresses the importance of microclimatic complexity for the persistence of biological assemblages under climate changes occurring over broad spatial scales[33]. We detected no clear effects of human population changes on functional β-diversity. Finally, assemblages showed contrasting responses to changes in natural habitats. The biological consequences of the increase in wild areas and forests are controversial[48], especially when re-wilding is unmanaged, human population density is high and there is a long history of intensive land-use, as often happens in European countries[60,61]. We found fast changes in taxonomic β-diversity and nestedness, and a fast functional turnover with increasing rates of re-wilding (Fig. 3a, c and e). This process mainly occurred by addition of species or functionality, rather than by species loss (Fig. 5a and c), confirming that the increase of resources availability in increasingly natural habitats can have profound effects on biodiversity, promoting the broad-scale recovery of functional diversity in a few decades[62].

The thorough quantification of temporal β-diversity at macroecological scales is generally hampered by the lack of data on assemblage composition, even on short time scales[17]. However, herbaria and zoological collections represent fundamental archives of biodiversity information[63] and historical data, spanning over the period of accelerated anthropogenic impact on ecosystems, allow the identification of the baseline levels of biodiversity and biodiversity trajectories. Ad-hoc assembled long-term distribution, climatic and trait datasets can allow the understanding of the complex processes shaping functional and taxonomic diversity following long-term environmental changes. In this way, we will be able to shed light into the mechanisms underlying the observed

functional and compositional changes, identifying the relative contributions of colonization and extinction in the biodiversity response to global scale drivers.

Methods

Biological models and data collection

Assemblage data were retrieved from a recently developed distribution dataset for the Italian fauna[30]. The initial dataset included 268,997 occurrence records from 8,445 species, dating between 1680 and 2006 CE. We considered a subset of this dataset, focusing on taxonomic groups and periods for which sample size is large enough to ensure robustness of analyses. We retained groups with: i) average number of records > 40 per each species; ii) > 25 species and iii) a high taxonomic coverage (> 85%) with respect to the updated checklist of the Italian fauna (http://www.faunaitalia.it/checklist/; accessed on 25 January 2019). We initially retained 18 taxonomic groups (122,438 dated records). Subsequently, we adopted a strict protocol to retain only the cells and periods that received a consistently high sampling effort. Within each taxonomic group we collapsed occurrence data using a spatio-temporal grid structure with 20 × 20 km cells and 10-year timeframes (hereafter assemblages), discarding all cells with fewer than 10 records. The number of observed species in a cell will likely be lower than the actual number of species because some species may remain undetected. To address this issue, several estimators of species richness have been developed[64]. These estimators use information on the number of rare species (i.e., species found only once or twice) in the assemblage. They assume that the greater the number of locally rare species is, the more likely it is that other species were missed, and hence they correct the observed richness based on the frequency of rare species[64,65]. For each assemblage, we built a matrix with occurrence records in rows and species in columns. We then estimated the species richness of the assemblage using the first-order jackknife estimation with the *specpool* function in *vegan*[66]. The first order jackknife is among the best performing approaches to estimate the

completeness of biodiversity inventories; simulations and analyses of real datasets of completely surveyed areas confirmed that it can provide robust estimates of the actual species richness [67]. In order to identify the assemblages where the majority of present species have been detected, we calculated the ratio between observed and estimated number of species for each assemblage. We retained for analyses only those assemblages with completeness (observed / estimated) > 0.6, i.e. assemblages where biodiversity data most likely represent > 60% of species that were actually present in a given period. To take into account the possibility that a proportion of the species pool may remain undetected within each assemblage, we included the estimates of completeness as model weights in later analyses, using the average value between each pair of assemblages. Including completeness as model weights gives more importance in regression analyses to the best-sampled assemblages, thus reducing the risk of incorrect or misleading model outputs. The completeness was rather homogeneous across assemblages (mean = 0.69; 5%-95% quantiles = 0.62-0.82) and assemblages surveyed in different periods generally showed consistent completeness (average within-pair difference = 0.07). We finally excluded all taxonomic groups with fewer than 5 cells × timeframes remaining, or with highly clustered distribution data (i.e., occupying only a small portion of the study area). After this cleansing, we retained three taxa of strictly terrestrial arthropods [Chilopoda (centipedes); Histeridae (clown beetles); and Orthoptera (grasshoppers and crickets)] and three taxa of amphibious insects [(Dytiscidae (water beetles); Ephemeroptera (mayflies); and Odonata (dragonflies)]. The final dataset comprised 169 pairs of assemblages, representing 631 species and 9,009 dated records spanning between 1859 and 2003. Each pair comprised two assemblages where the same taxonomic group was sampled in the same cell in different time frames with high sampling intensity; 34% of pairs had at least one assemblage dating before 1960 CE. The duration of the interval between sampling occasions varied from 10 to 110 years. Differences in the spatial representativeness between samples from the same assemblage may potentially bias the measurement of biodiversity changes[16]. Following Marta et al.[30], we used Voronoi cells to evaluate the spatial grain of observation for each sampling locality (and the

associated records). For each record in each assemblage, we measured the distance between the centroid and the vertices of the respective Voronoi cell, and then calculated the standard variation of this distance between all the records of each assemblage. For 90% of assemblages, this standard deviation was ≤ 618 m, with a within-cell range of deviations between timeframes < 563 m, suggesting that the grain of records is homogeneous and much finer than the size of cells.

For each species, we searched for traits covering the major features of organismal biology[68]: i) morphology (adult body size); ii) feeding (feeding guild and foraging strategies); iii) life history (life style, life span, age at maturity); iv) behaviour (daily activity, dispersal mode and annual activity) and v) ecology (specialization). Several sources were consulted (see Supplementary Note 1 and Supplementary Table 2 for further details), but we were unable to collect satisfactory information for all traits. We thus retained six traits: adult size (continuous), feeding guild and foraging strategies (categorical; 9 and 4 levels, respectively), life style (categorical; amphibian or not), dispersal mode (categorical; 3 levels) and habitat specialization (continuous; N habitats used by each species / N habitats used by the whole taxonomic group) (Supplementary Note 1 and Supplementary Table 2). Categorical variables with more than two levels where then expressed as trait carried / not carried by the i^{th} species. The resulting dataset showed a high completeness (98.54%; 264 NAs); missing data were imputed using recursive partitioning in *mice*[69]; given the lack of sequence-based phylogenies, we included phylogenetic information in the form of taxonomic hierarchy (taxonomic group + genus + subgenus, if any) to obtain more robust trait predictions.

Climate, land-use and human population changes

The climate information provided by widely used global datasets of centennial meteorological series often lack representativeness at local scales. This issue is particularly relevant in orographically complex regions. For this reason, we reconstructed the climate information for each cell in a more accurate way by exploiting the instrumental data available for Italy beginning in the

18th century[39]. This guarantees a level of data availability that is one to two orders of magnitude larger than the number of stations usually considered in the global datasets[70].

For each assemblage, we reconstructed mean monthly temperature and total monthly precipitation of the cell centroid, using the average cell elevation and applying the anomaly method[71] to the time series of meteorological variables, as described in Brunetti et al.[72]. A time series of a meteorological variable can be described as the superposition of the climatology (i.e., the climate normals over a given reference period, which is assumed to be constant through time), and the deviations from them (i.e., the anomalies with respect to the same period, which define how much a given month deviates from its typical value). The anomaly approach consists of the independent reconstruction of these two components. Climatologies can show remarkable spatial gradients, reflecting the geographical features of the area, such as elevation or topography. Consequently, the spatial interpolation of climate normals requires a weather station network with high spatial density. For each cell, we reconstructed the climate normals referred to the period 1961-1990 CE (the period with the highest data availability) based on the most representative nearby stations (a minimum of 15 and a maximum of 35 stations were retained). This was obtained through a weighted linear regression of the meteorological variable versus elevation, by assigning larger weights to the stations with elevation and topographic parameters similar to those of the cell of interest, as derived from a 30 arc-second resolution digital elevation model[73,74]. Anomalies are linked to climate variability and climate change through time, and show higher spatial coherence. Therefore, a limited number of weather stations can be sufficient to capture the spatial patterns, but a long temporal coverage and an accurate homogenization of the time series are essential[75]. Consequently, we i) removed non-climatic signals due to the history of the stations (e.g. instrument relocation or changes in measurement practices); ii) calculated the monthly anomalies with respect to 1961-1990 CE and iii) linearly interpolated on the coordinate of the cell of interest through a weighted average of the anomalies of nearby stations . Quantitative monthly temperature and precipitation series for each location were then estimated by superposing climatologies and

anomalies. Finally, mean annual temperature and total annual precipitation were calculated for each year and aggregated over the 10-year timeframe of interest. All validation analyses returned a high accuracy of this approach[72,73,74].

Land-use and human population density data were retrieved from the HYDE 3.2.1 dataset at 5 arc-minutes resolution[47]. For each assemblage, we extracted estimates of human population density (inhabitants / km^2) and natural habitats. The percent of natural habitat in each cell was obtained as the area not covered by croplands, grazing and built-up areas, divided by the total available land area. Note that this also includes semi-natural habitats such as managed forests. Precipitation and human population data were cube-root transformed to increase normality and the independent variable (i.e. year) was scaled to zero mean and unit variance before modelling. We used linear mixed models (LMMs) to explore the pattern of environmental change through time. We built LMMs with temperature, precipitation, natural habitat and human population as dependent variables and year as the independent variable. Models were fitted in *lme4*[76], with a random intercept on grid cell identity. For each dependent variable, models with linear, quadratic and exponential relationships between the variable and year were compared, and the model with the lowest value of the Akaike information criterion (AIC) was selected[77].

Calculating temporal β-diversity

Temporal changes in assemblage composition and functionality were estimated using the Sørensen dissimilarity between pairs of temporally disjunct assemblages from the same taxonomic group and cell ($\beta_{sor} = \frac{b+c}{2a+b+c}$), where a is the number of species that persisted between t_0 and t_1, b is the number of species that colonized and c the number of species that went locally extinct. Temporal β-diversities were also partitioned in their additive nestedness and turnover components[19]. Temporal turnover ($\beta_{sim} = \frac{\min(b,c)}{a+\min(b,c)}$) reflects species replacement over time, while temporal nestedness

($\beta_{sne} = \frac{\max(b,c)-\min(b,c)}{2a+b+c} \times \frac{a}{a+\min(b,c)} = \beta_{sor}-\beta_{sim}$) is the tendency of two assemblages to be subset of one another[19,20].

We further decomposed the Sørensen dissimilarity into scaled gain and loss components (D_{gain} and D_{loss}[32]). These terms correspond to the $\frac{b}{2a+b+c}$ and $\frac{c}{2a+b+c}$ components of Sørensen, respectively, so that they sum up to β. In a temporal perspective, loss and gain components can be directly linked to extinction and colonization, given that *b* and *c* represent the number of species occupying the same site in t_0 but not in t_1 and vice versa, respectively. In the case of cells with assemblage data for more than two time periods for a taxonomic group (e.g. t_0, t_1 and t_2), we calculated dissimilarity indices sequentially (e.g., t_0 to $t1$ and then t_1 to t_2) and treated each measure as a distinct value. For taxonomic dissimilarity we used the number of shared, colonizing and extinct species between t_0 and t_1. For functional dissimilarity, we replaced the number of species with the functional diversity associated to shared, colonizing and extinct species, when calculating functional indices[16]. The functional trait space occupied by each assemblage was calculated using hypervolumes with Gaussian kernel density estimation in *hypervolume*[78]. Components entering the hypervolume calculation must be centred, scaled, continuous and uncorrelated, and should not exceed 5-8 to avoid disjunct hypervolumes (i.e., a great number of holes)[79]. When dealing with possibly correlated and / or categorical traits, principal coordinates analysis (PCoA) based on pairwise trait dissimilarities allows one to reduce dimensionality and obtain orthogonal, centred and scaled components[80]. Trait dissimilarities were calculated using Gower distances in *FD*[81], with equal weights to each trait (i.e., down-weighting categorical traits based on their number of levels); Gower distances are indeed appropriate to handle both quantitative and qualitative variables[81]. We computed PCoAs separately for each taxonomic group and retained the number of axes explaining at least 90% of the variance within each group (Chilopoda: 4 axes; Histeridae: 4; Orthoptera: 5; Dytiscidae: 5; Ephemeroptera: 4; Odonata: 3). Factor scores from the retained axes were then treated as the new trait values, and used to build hypervolumes for each assemblage. Within each

pair of assemblages (same cell and taxonomic group, but different timeframes), functional diversities associated to shared, colonizing and extinct species were obtained by calculating the intersection (shared) and the unique components (colonizing and extinct) of the two hypervolumes. Since functional diversity is highly sensitive to species richness, we used null models to obtain estimates of functional diversity uncorrelated to species richness[36,37]. Within each taxonomic group, we shuffled the species names 500 times in the PCoA-based trait matrix, and recalculated all functional indices (β_{sor}, β_{sim}, β_{sne}, D_{gain} and D_{loss}; 5 indices × 169 pairs of assemblages). Name shuffling is preferred to the 'independent swap' (i.e., a constrained randomization of the community matrix) when dealing with β–diversity, as it allows the maintaining of the overall spatial pattern of richness and trait covariance[37]. Standardized effect size (SES) is a commonly applied method to measure the departures of the observed index from the null distribution[37], but SES comparisons can produce biased inferences if null indices have a non-normal or asymmetric distribution[82]. None of the null indices showed a normal distribution (Shapiro-Wilk test: all $P < 0.05$) and the *Skew* test in *DescTools*[83] (500 bootstrap replicates per index) showed that 97% of the null distributions were skewed. Consequently, we estimated P-values using quantile scores for each null distribution, and used these values as measures of effect size[37,82]. This approach is known to partially underestimate the size of the effect when the observed index is completely outside the null distribution (i.e., P = 0 or 1), however this issue did not affect our analysis as just 2.6% of our measures returned values of 0 or 1.

Average rates of change for β–diversity, turnover, nestedness and scaled components of β–diversity were obtained by dividing the indices by the length of the interval over which they were measured. For taxonomic diversity, this allowed maintaining the additive properties for both nestedness and turnover ($\beta_{sor}' = \beta_{sne}' + \beta_{sim}'$) and D_{gain} and D_{loss} ($\beta_{sor}' = D_{gain}' + D_{loss}'$).

Modelling β–diversity change over time

To measure changes of climate, land-use and human population density for each pair of assemblages, we used the difference in the value of variables; for pairs of assemblages with sampling occasions at intervals >10 years (i.e. interval duration 20 years or more), we used the difference between the values from the last and the first decade. As above, annual rates of change for climate, land-use and human population density were obtained by dividing the overall change by the duration of the interval. Suggitt et al.[33] proposed that microclimatically heterogeneous landscapes may buffer local assemblages against extinction; we therefore calculated microclimatic heterogeneity as the standard deviation in the solar index over the decade of interest for each 20 km cell using the *solarindex* function[84]. We generated the slope and aspect data needed to calculate the solar index from the SRTM digital elevation model, aggregated at the 9 arc-second resolution. The mean value between the two time points of each interval was taken as the average microclimatic heterogeneity over the cell and the timeframe of interest. The rate of change of human population density and the average microclimatic heterogeneity data were cube-root transformed to increase normality and all variables were scaled to zero mean and unit variance before analyses. Correlation between pairs of environmental variables was weak (in all pairwise correlations, $|r| \leq 0.45$), indicating that multicollinearity did not pose problems to our models. Consequently, for each pair of assemblages (same cell and taxonomic group, different timeframes), we had 10 measures of β-diversity (five taxonomic and five functional), and five predictors: annual rates of change of temperature, precipitation, population density and % natural habitat, and the average microclimatic heterogeneity.

We used Bayesian generalized linear mixed models (GLMMs) to identify the processes shaping β-diversity and its components, while taking into account the complex spatial structure of the dataset. For both taxonomic and functional diversity, we considered five dependent variables describing temporal changes in diversity: β-diversity, nestedness, turnover, D_{gain} and D_{loss}. The dependent variables were related to the five independent variables. In GLMMs, taxonomic group was used as random intercept. We then used a conditional autoregressive term to account for spatial

autocorrelation. Spatial autocorrelation occurs when nearby localities have similar values for a given parameter, and ignoring the dependence structure arising from spatially autocorrelated data may result in biased estimates of the model parameters[85]. We thus introduced a spatial random effect using the Besag spatial model[86] to take into account the non-independence between nearby cells. We measured spatial dependence through a binary neighbourhood matrix, calculated in *spdep*[87]; all the cells within 90 km from each other were treated as neighbours. The different cells received uneven sampling efforts, and the available data have variable completeness. Therefore, in mixed models we also included as weights the average taxonomic completeness of the pair of assemblages for which we calculated dissimilarity. We fitted Bayesian GLMMs using integrated nested Laplace approximation with default priors, as implemented in *INLA*[88,89]. INLA allows reliably approximating posterior marginals in models with complex spatial structures, while considerably reducing computational load and solving convergence issues[88]. The responses were bounded on the closed interval [0,1], thus we first removed fixed zeros and ones by taking $y' = \frac{y \times (N-1) + 0.5}{N}$, where N is the sample size[90], and then fit GLMMs with beta family. To take into account the possibility of non-linear relationships, we ran five models for both taxonomic and functional β-diversity (β_{sor}), either including or excluding quadratic terms for changes in climate, land-use and human population density. We also tested the possibility of interactions between parameters representing climate change (temperature × precipitation) and between climate and land-use change (temperature or precipitation × human population or natural habitat). In the final models for taxonomic and functional β_{sor}, we included all the linear terms, and all those quadratic terms and interactions that reduced the Watanabe-Akaike information criterion (WAIC[35]). The retained terms were then applied to all the components of diversity (β_{sne}, β_{sim}, D_{gain} and D_{loss}). All the analyses were performed with R v.4.0.3[91].

References

1. Newbold, T. Future effects of climate and land-use change on terrestrial vertebrate community diversity under different scenarios. *Proc. R. Soc. B* **285,** 20180792 (2018).

2. Peters, M. K. et al. Climate-land-use interactions shape tropical mountain biodiversity and ecosystem functions. *Nature* **568,** 88-92 (2019).

3. Ellis, E. C., Klein Goldewijk, K., Siebert, S., Lightman, D. & Ramankutty, N. Anthropogenic transformation of the biomes, 1700 to 2000. *Global Ecol. Biogeogr.* **19,** 589-606 (2010).

4. Newbold, T. et al. Global effects of land use on local terrestrial biodiversity. *Nature* **520,** 45-50 (2015).

5. Parmesan, C. Ecological and evolutionary responses to recent climate change. *Annu. Rev. Ecol. Evol. Syst.* **37,** 637-669 (2006).

6. Scheffers, B. R. et al. The broad footprint of climate change from genes to biomes to people. *Science* **354,** aaf7671 (2016).

7. Mantyka-Pringle, C. S., Martin, T. G. & Rhodes, J. R. Interactions between climate and habitat loss effects on biodiversity: a systematic review and meta-analysis. *Global Change Biol.***18,** 1239-1252 (2012).

8. Falaschi, M., Manenti, R., Thuiller, W. & Ficetola, G.F. Continental-scale determinants of population trends in European amphibians and reptiles. *Global Change Biol.* **25,** 3504-3515 (2019).

9. Cardinale, B. J. et al. Biodiversity loss and its impact on humanity. *Nature* **486,** 59-67 (2012).

10. Pecl, G. T. et al. Biodiversity redistribution under climate change: impacts on ecosystems and human well-being. *Science* **355,** eaai9214 (2017).

11. Jarzyna, M. A. & Jetz, W. Detecting the multiple facets of biodiversity. *Trends Ecol. Evol.* **31,** 527- 538 (2016).

12. Hanson, J. O. et al. Global conservation of species' niches. *Nature* **580,** 232-234 (2020).

13. Bell, J. R. et al. Spatial and habitat variation in aphid, butterfly, moth and bird phenologies over the last half century. *Global Change Biol.* **25,** 1982-1994 (2019).
14. Finderup Nielsen, T., Sand-Jensen, K., Dornelas, M. & Bruun, H. H. More is less: net gain in species richness, but biotic homogenization over 140 years. *Ecol. Lett.* **22,** 1650-1657 (2019).
15. van Strien, A. J., van Swaay, C. A., van Strien-van Liempt, W. T., Poot, M. J. & WallisDeVries, M. F. Over a century of data reveal more than 80% decline in butterflies in the Netherlands. *Biol. Conserv.* **234,**116-122 (2019).
16. Jarzyna, M. A. & Jetz, W. Taxonomic and functional diversity change is scale dependent. *Nat. Commun.* **9,** 2565 (2018).
17. Magurran, A. E., Dornelas, M., Moyes, F. & Henderson, P. A. Temporal β diversity-A macroecological perspective. *Global Ecol. Biogeogr.* **28,** 1949-1960 (2019).
18. Dornelas, M. et al. Assemblage time series reveal biodiversity change but not systematic loss. *Science* **344,** 296-299 (2014).
19. Baselga, A. Partitioning the turnover and nestedness components of beta diversity. *Global Ecol. Biogeog.* **19,** 134-143 (2010).
20. Baselga, A. The relationship between species replacement, dissimilarity derived from nestedness, and nestedness. *Global Ecol. Biogeogr.* **21,** 1223-1232 (2012).
21. Kondratyeva, A., Grandcolas, P. & Pavoine, S. Reconciling the concepts and measures of diversity, rarity and originality in ecology and evolution. *Biol. Rev.* **94,** 1317-1337 (2019).
22. Auffret, A. G. & Thomas, C. D. Synergistic and antagonistic effects of land use and non-native species on community responses to climate change. *Global Change Biol.* **25,** 4303-4314 (2019).
23. WallisDeVries, M. F. & van Swaay, C. A. A nitrogen index to track changes in butterfly species assemblages under nitrogen deposition. *Biol. Conserv.* **212**, 448-453 (2017).
24. Zellweger, F. et al. Forest microclimate dynamics drive plant responses to warming. *Science* **368**, 772-775 (2020).

25. Sgardeli, V., Zografou, K. & Halley, J. M. Climate change versus ecological drift: assessing 13 years of turnover in a butterfly community. *Basic. Appl. Ecol.* **17,** 283-290(2016).
26. van Klink, R. et al. Meta-analysis reveals declines in terrestrial but increases in freshwater insect abundances. *Science* **368,** 417-420 (2019).
27. Seibold, S., et al. Arthropod decline in grasslands and forests is associated with landscape-level drivers. *Nature* **574,** 671-674 (2019).
28. Outhwaite, C. L., Gregory, R. D., Chandler, R. E., Collen, B. & Isaac, N. J. B. Complex long-term biodiversity change among invertebrates, bryophytes and lichens. *Nat. Ecol. Evol.* **4,** 384-392 (2020).
29. Soroye, P., Newbold, T. & Kerr, J. Climate change contributes to widespread declines among bumble bees across continents. *Science* **367,** 685-688 (2020).
30. Marta, S. et al. ClimCKmap, a spatially, temporally and climatically explicit distribution database for the Italian fauna. *Sci. Data* **6,** 195 (2019).
31. Koleff, P., Gaston, K. J. & Lennon, J. T. Measuring beta diversity for presence-absence data. *J. Anim. Ecol.* **72,** 367-382 (2003)
32. Legendre, P. A temporal beta-diversity index to identify sites that have changed in exceptional ways in space–time surveys. *Ecol. Evol.* **9,** 3500-3514 (2019).
33. Suggit, A. J. et al. Extinction risk from climate change is reduced by microclimatic buffering. *Nat. Clim. Change* **8,** 713-717 (2018).
34. Baselga, A., Bonthoux S., & Balent, G. Temporal beta diversity of bird assemblages in agricultural landscapes: land cover change vs. stochastic processes. *PloS One* **10,** e0127913 (2015).
35. Watanabe, S. Asymptotic equivalence of Bayes cross validation and widely applicable information criterion in singular learning theory. *J. Mach. Learn. Res.* **11,** 3571-3594 (2010).

620 36. Mason, N. W., de Bello, F., Mouillot, D., Pavoine, S. & Dray, S. A guide for using functional
621 diversity indices to reveal changes in assembly processes along ecological gradients. *J. Veg.*
622 *Sci.* **24,** 794-806 (2013).
623 37. Swenson, N. G. *Functional and phylogenetic ecology in R*. (Springer, New York, 2014).
624 38. Giorgi, F. & Lionello, P. Climate change projections for the Mediterranean region. *Global*
625 *Planet. Change* **63,** 90-104(2008).
626 39. Brunetti, M., Maugeri, M., Monti, F. & Nanni, T. Temperature and precipitation variability in
627 Italy in the last two centuries from homogenised instrumental time series. *Int. J. Climatol.* **26,**
628 345-381 (2006).
629 40. Terzago, S., von Hardenberg, J., Palazzi, E. & Provenzale, A. Snow water equivalent in the
630 Alps as seen by gridded data sets, CMIP5 and CORDEX climate models. *The Cryosphere* **11,**
631 1625-1645 (2017).
632 41. Beniston, M. et al. The European mountain cryosphere: A review of its current state, trends and
633 future challenges. *The Cryosphere* **12,** 759-794 (2018).
634 42. Wang, J. et al. Anthropogenically-driven increases in the risks of summertime compound hot
635 extremes. *Nat. Commun.* **11,** 528 (2020).
636 43. Turco, M. et al. Exacerbated fires in Mediterranean Europe due to anthropogenic warming
637 projected with nonstationary climate-fire models. *Nat. Commun.* **9,** 3821(2018).
638 44. Jacobson, A. R., Provenzale, A., von Hardenberg, A., Bassano, B. & Festa-Bianchet, M.
639 Climate forcing and density dependence in a mountain ungulate population. *Ecology* **85,**
640 1598-1610 (2004).
641 45. Imperio, S., Bionda, R., Viterbi, R. & A. Provenzale. Climate change and human disturbance
642 can lead to local extinction of Alpine rock ptarmigan: new insight from the Western Italian
643 Alps. *PloS One* **8,** e81598 (2013).
644 46. Hoffmann, S., Beierkuhnlein, C., Field, R., Provenzale, A. & Chiarucci, A. Uniqueness of
645 protected areas for conservation strategies in the European Union. *Sci. Rep.* **8,** 6445 (2018).

646 47. Klein Goldewijk, K., Beusen, A., Doelman, J. & Stehfest, E. Anthropogenic land use estimates
647 for the Holocene - HYDE 3.2. *Earth Syst. Sci. Data* **9,** 927-953 (2017).
648 48. Queiroz, C., Beilin, R., Folke, C. & Lindborg, R. Farmland abandonment: threat or opportunity
649 for biodiversity conservation? A global review. *Front. Ecol. Environ.* **12,** 288-296 (2014).
650 49. Falcucci, A., Maiorano, L. & Boitani, L. Changes in land-use/land-cover patterns in Italy and
651 their implications for biodiversity conservation. *Landscape Ecol.* **22,** 617-631(2007).
652 50. Gerland, P. et al. World population stabilization unlikely this century. *Science* **346,** 234-237
653 (2014).
654 51. Ranganathan, S., Swain, R. B. & Sumpter, D. J. T. The demographic transition and economic
655 growth: implications for development policy. *Palgrave Commun.* **1,** 15033 (2015).
656 52. Weltzin, J. F. et al. Assessing the response of terrestrial ecosystems to potential changes in
657 precipitation. *BioScience* **53,** 941-952 (2003).
658 53. Lacasella, F. et al. From pest data to abundance-based risk maps combining eco-physiological
659 knowledge, weather, and habitat variability. *Ecol. Appl.* **27,** 575-588 (2017).
660 54. Ficetola, G. F. & Maiorano, L. Contrasting effects of temperature and precipitation change on
661 amphibian phenology, abundance and performance. *Oecologia* **181,** 683-693 (2016).
662 55. Crimmins, S. M., Dobrowski, S. Z., Greenberg, J. A., Abatzoglou, J. T. & Mynsberge, A. R.
663 Changes in climatic water balance drive downhill shifts in plant species' optimum elevations.
664 *Science* **331,** 324-327 (2011).
665 56. Adams, H. D. et al. Temperature sensitivity of drought-induced tree mortality portends
666 increased regional die-off under global-change-type drought. *Proc. Natl. Acad. Sci. USA* **106,**
667 7063-7066 (2009).
668 57. Cahill, A. E. et al. How does climate change cause extinction?. *Proc. R. Soc. B* **280,** 20121890
669 (2013).
670 58. Brook, B. W., Sodhi, N. S. & Bradshaw, C. J. Synergies among extinction drivers under global
671 change. *Trends Ecol. Evol.* **23,** 453-460 (2008).

59. Poff, N. L. et al. Sustainable water management under future uncertainty with eco-engineering decision scaling. *Nat. Clim. Change* **6,** 25-34 (2017).

60. Corlett, R. T. Restoration, reintroduction, and rewilding in a changing world. *Trends Ecol. Evol.* **31,** 453-462 (2016).

61. Kremen, C. & Merenlender, A. M. Landscapes that work for biodiversity and people. *Science* **362**, eaau6020 (2018).

62. Galland, T. et al. Colonization resistance and establishment success along gradients of functional and phylogenetic diversity in experimental plant communities. *J. Ecol.* **107,** 2090-2104 (2019).

63. Lister, A. M. et al. Natural history collections as sources of long-term datasets. *Trends Ecol. Evol.* **26,** 153-154 (2011).

64. Colwell, R. K. & Coddington, J. A. Estimating terrestrial biodiversity through extrapolation. *Phil. Trans. R. Soc. Lond. B* **345,** 101-118 (1994).

65. Gotelli, N. J. & Colwell, R. K. Quantifying biodiversity: procedures and pitfalls in the measurement and comparison of species richness. *Ecol. Lett.* **4,** 379-391 (2001).

66. Oksanen, J. et al. *vegan: Community Ecology Package*. R package version 2.5-6 (2019).

67. Chazdon, R. L., Colwell, R. K., Denslow, J. S. & Guariguata, M.R. Statistical methods for estimating species richness of woody regeneration in primary and secondary rain forests of northeastern Costa Rica. (1998). In: *Forest biodiversity research, monitoring and modeling: Conceptual background and Old World case studies*, 285-309 (Parthenon Publishing, Paris, 1998).

68. Moretti, M. et al. Handbook of protocols for standardized measurement of terrestrial invertebrate functional traits. *Funct. Ecol.* **31,** 558-567 (2017).

69. van Buuren, S. & Groothuis-Oudshoorn, K. mice: multivariate imputation by chained equations in R. *J. Stat. Softw.* **45,** 1-67 (2011).

70. Osborn, T. J. & Jones, P. The CRUTEM4 land-surface air temperature data set: construction, previous versions and dissemination via Google earth. *Earth Syst. Sci. Data* **6,** 61-68 (2014).
71. New, M., Hulme, M. & Jones, P. Representing twentieth-century space-time climate variability. Part II: development of 1901–96 monthly grids of terrestrial surface climate. *J. Clim.* **13,** 2217-2238 (2000).
72. Brunetti, M. et al. Projecting north eastern Italy temperature and precipitation secular records onto a high resolution grid. *Phys. Chem. Earth* **40,** 9-22 (2012).
73. Brunetti, M., Maugeri, M., Nanni, T., Simolo, C. & Spinoni, J. High-resolution temperature climatology for Italy: interpolation method intercomparison. *Int. J. Climatol.* **34,** 1278-1296 (2014).
74. Crespi, A., Brunetti, M., Lentini, G. & Maugeri, M. 1961-1990 high-resolution monthly precipitation climatologies for Italy. *Int. J. Climatol.* **38,** 878-895 (2018).
75. Peterson, T. C. et al. Homogeneity adjustments of in situ atmospheric climate data: a review. *Int. J. Climatol.* **18,** 1493-1517 (1998).
76. Bates, D., Mächler, M., Bolker, B. & Walker, S. Fitting linear mixed-effects models using lme4. *J. Stat. Softw.* **67,** 1-48 (2015).
77. Burnham, K. & Anderson, D. *Model selection and multi-model inference*. (Springer, New York, 2002).
78. Blonder, B & Harris, D. J. *hypervolume: High Dimensional Geometry and Set Operations Using Kernel Density Estimation, Support Vector Machines, and Convex Hulls*. R package version 2.0.12 (2019).
79. Blonder, B., Lamanna, C., Violle, C. & Enquist, B. J. The n-dimensional hypervolume. *Global Ecol. Biogeogr.* **23,** 595-609 (2014).
80. Barros, C., Thuiller, W., Georges, D., Boulangeat, I. & Münkemüller, T. N-dimensional hypervolumes to study stability of complex ecosystems. *Ecol. Lett.* **19,** 729-742 (2016).

722 81. Laliberté, E. & Legendre, P. A distance-based framework for measuring functional diversity
723 from multiple traits. *Ecology* **91,** 299-305 (2010).
724 82. Botta-Dukát, Z. Cautionary note on calculating standardized effect size (SES) in randomization
725 test. *Community Ecol.* **19,** 77-83 (2018).
726 83. Signorell, A. et al. *DescTools: Tools for descriptive statistics*. R package version 0.99.40
727 (2021).
728 84. Maclean, I. M. D., Suggitt, A. J., Wilson, R. J., Duffy, J. P. & Bennie, J. J. Fine-scale climate
729 change: modelling fine-scale spatial variation in biologically meaningful rates of warming.
730 *Global Change Biol.* **23,** 256-268 (2017).
731 85. Dormann, C. F. et al. Methods to account for spatial autocorrelation in the analysis of species
732 distributional data: a review. *Ecography* **30,** 609-628 (2007).
733 86. Besag, J., York, J. & Mollié, A. Bayesian image restoration, with two applications in spatial
734 statistics. *Ann. Inst. Stat. Math.* **43,** 1-20 (1991).
735 87. Bivand, R. S. & Wong, D. W. Comparing implementations of global and local indicators of
736 spatial association. *Test* **27,** 716-748 (2018).
737 88. Rue, H., Martino, S. & Chopin, N. Approximate Bayesian inference for latent Gaussian models
738 by using integrated nested Laplace approximations. *J. R. Stat. Soc. B* **71,** 319-392 (2009).
739 89. Bivand, R. S., Gómez-Rubio, V. & Rue, H. Spatial data analysis with R-INLA with some
740 extensions. *J. Stat. Softw.* **63,** 1-31 (2015).
741 90. Smithson, M. & Verkuilen, J. A better lemon squeezer? Maximum-likelihood regression with
742 beta-distributed dependent variables. *Psychol. Methods* **11,** 54-71 (2006).
743 91. R Core Team. *R: A language and environment for statistical computing*. (R Foundation for
744 Statistical Computing, Vienna, 2020).
745 92. Nakagawa, S. & Schielzeth, H. A general and simple method for obtaining R^2 from generalized
746 linear mixed-effects models. *Methods Ecol. Evol.* **4,** 133-142 (2013).

Acknowledgements

We are grateful to two reviewers and David O'Brien for the revision of an early version of the manuscript. S.M. and G.F.F. are funded by the European Research Council under the European Community's Horizon 2020 Programme, Grant Agreement No. 772284 ('IceCommunities - Reconstructing community dynamics and ecosystem functioning after glacial retreat').

Author Contributions

SM, GFF and RM designed the study. MB and AP associated climatic information to each distribution record, while SM retrieved distribution and trait data and performed the analyses. SM and GFF led the writing with substantial contributions from all the other authors.

Competing Interests statement

The authors declare no competing interests

Figure Legends

Fig. 1: Potential effects of environmental changes on the α- and β-diversity of assemblages. The effects are exemplified for two assemblages sharing the same pool of species at t_1, but experiencing different intensities of change. a) An environmental change leads to a modification in assemblage composition between t_1 and t_2, with stronger environmental change for the blue assemblage. b): These environmental changes affect biodiversity, leading to loss of α-diversity (strongest for the blue assemblage) and causing higher temporal β-diversity (β_{sor}) in blue, which is attributable to nestedness (β_{sne}). c) In this case, the environmental change causes assemblage modifications that, as shown in d), are reflected by higher temporal β-diversity (β_{sor}) in blue, attributable to turnover (β_{sim}). e-g): For many parameters, the environment can drive changes with different sign (e.g. precipitation can either increase and decrease through time; Fig. 2b), both causing community

772 changes. As shown in f-h), this leads to non-linear relationships between the strength of
773 environmental change and the different components of β-diversity.
774
775 Fig. 2: Temporal evolution of climate, land-use and human population density over the entire time
776 series (1859-2003 CE). Cell identity was introduced as random intercept to take into account the
777 cell-specific conditions influencing climate (e.g., elevation, latitude ...), land-use and human
778 population density (percentage of natural areas or human population density at the beginning of the
779 series). a-d: reconstructed temporal trends (Nakagawa & Schielzeth[92] conditional R^2: 0.99; 0.96;
780 0.97; 0.99 - marginal R^2: 0.02, 0.01, 0.03, 0.02); grey area represents the 95% confidence interval
781 for the average estimate. Precipitation and human population density are cube-root transformed. e-
782 h: spatial distribution of the random intercepts; purple squares mark negative values (i.e. lower than
783 the average), green squares positive ones. The square size is proportional to the value of the random
784 intercept.
785
786 Fig. 3: Density plots of the posterior distribution for the relationships between the rates of change of
787 β-diversity, turnover and nestedness and the candidate environmental drivers. Taxonomy (a-c) vs.
788 functionality (d-f); Sørensen dissimilarity (a and d), temporal turnover (b and e), and temporal
789 nestedness (c and f). The figure represents median values for regression coefficients (vertical lines),
790 and 80 (colours), 95 (pale colours) and 99 % (outlines) credible intervals. Quadratic terms and
791 interactions were only included if supported for β_{Sor} by the Watanabe-Akaike Information
792 Criterion[35]. Interactions: Prec = Annual precipitation; H pop = Human population density; Temp =
793 mean annual temperature.
794
795 Fig. 4: Relationships between β-diversity and the environmental drivers returning significant
796 interactions. In each plot, the thick red line represents the average predicted relationship on the link

scale, while the grey lines represent 500 samples of the posterior distribution. a-c show the effect of precipitation change (mm/year) on taxonomic β-diversity in cells with negative (-0.45), medium (0.72) and rapid (1.82) changes of the human population density (cube-root transformed; (inhabitants/km^2/year)$^{1/3}$). d-f show the effect of temperature change (°C/year) on functional β-diversity with negative (-10.06), stable (-1.96) and positive (5.4) rates of change in precipitation (mm/year).

Fig. 5: Density plots of the posterior distribution for the relationships between the rates of change in the scaled gain (D_{gain}) and loss (D_{loss}) components of β-diversity and candidate environmental drivers. Taxonomy (a-b) vs. functionality (c-d); D_{gain} (a and b) and D_{loss} (c and d). The figure represents median values for regression coefficients (vertical lines), and 80 (colours), 95 (pale colours) and 99 % (outlines) credible intervals. Interactions: Prec = Annual precipitation; H pop = Human population density; Temp = mean annual temperature.

Supplementary information

Supplementary Fig. 1: Relationships between the rate of change of precipitation at slower, medium and faster changes of the human population density and taxonomic indices (β_{sim}, β_{sne}, D_{gain}, D_{loss}.)

Supplementary Fig. 2: Relationships between the rate of change of temperature with negative, stable and positive rate of changes of precipitation and functional indices (β_{sim}, β_{sne}, D_{gain}, D_{loss}.)

Supplementary Note 1: Structure and sources for the trait dataset (Supplementary Table 2).

Supplementary Table 1: Output of the linear mixed models used to reconstruct the temporal evolution of climate, land-use and human population density.

Supplementary Table 2: Trait dataset.